Earthquakes and Structures, *Vol. 13, No. 1 (2017) 000-000*
DOI: https://doi.org/10.12989/eas.2017.13.1.000

Parametric study of pendulum type dynamic vibration absorber for controlling vibration of a two DOF structure

Mulyadi Bur*[1], Lovely Son[1a], Meifal Rusli[1b] and Masaaki Okuma[2c]

[1]*Department of Mechanical Engineering, Faculty of Engineering, Andalas University, Kampus Limau Manis 25163, Indonesia*
[2]*Department of Mechanical and Aerospace Engineering, Tokyo Institute of Technology, Japan*

(Received October 30, 2016, Revised June 7, 2017, Accepted June 10, 2017)

Abstract. Passive dynamic vibration absorbers (DVAs) are often used to suppress the excessive vibration of a large structure due to their simple construction and low maintenance cost compared to other vibration control techniques. A new type of passive DVA consists of two pendulums connected with spring and dashpot element is investigated. This research evaluated the performance of the DVA in reducing the vibration response of a two degree of freedom shear structure. A model for the two DOF vibration system with the absorber is developed. The nominal absorber parameters are calculated using a Genetic Algorithm(GA) procedure. A parametric study is performed to evaluate the effect of each absorber parameter on performance. The simulation results show that the optimum condition for the absorber frequencies and damping ratios is mainly affected by pendulum length and mass, and the damping coefficient of the pendulum's hinge joint. An experimental model validates the theoretical results. The simulation and experimental results show that the proposed technique is able be used as an effective alternative solution for reducing the vibration response of a multi degree of freedom vibration system.

Keywords: vibration; structure; damping; building; earthquake

1. Introduction

In comparison with a one degree of freedom structure, a multi degree of freedom (MDOF) structure is more sensitive to dynamic loads such as the wind and seismic excitation (Wang *et al*. 2015 and Salazar *et al*. 2016). The reason is that MDOF structure generally has lower stiffness and a less inherent damping in comparison to a single degree of freedom(SDOF) structures. This kind of structures has a number of natural frequencies each with a corresponding mode shape. If this structure is excited by a dynamic load, then it will vibrate most strongly whenever the excitation frequency is closest to a natural frequency. This resonance phenomena induce an excessive dynamic bending moment and generates dynamic stress at the structure foundation.

Several techniques have been proposed to reduce the vibrations of a multi degree of freedom structure. Increasing the structural stiffness and damping by retrofitting the structure using stiffener and damping elements is one common method for reducing the vibration response of small and medium size structures (Ni 2014, Bayramoglu *et al.* 2014 and Zhang *et al.* 2015). However, for a large size structure such as a multi storey building, this method is costly and not effective because it needs several large damper elements to be installed.

Active vibration control methods have been proposed by several researchers for reducing the vibration response of MDOF vibration systems (Shariatmadar and Razavi 2014 and Gong *et al.* 2012). These can more effectively reduce the structure's response than a passive control method. However, there are several problems. The main problem is that this method needs electricity for the actuator and sensors to achieve good control performance.

Application of DVAs for reducing the response of a vibration system has been extensively developed by many researchers. Some methods from many literatures are focused to suppress the vibration response near the fundamental frequency of a vibration system. Application of a dynamical damper with a smart element using piezoelectric material was studied by Yamada (2015). Mizuno and Araki (1993) have studied the effectiveness of the dynamic vibration absorber with an electromagnetic servomechanism. Rosdick and Ketema have used the thermoviscoelastic material to tune the energy dissipation of a dynamic vibration absorber (1998). Optimum design and application of non-traditional tuned mass damper toward the seismic response control with experimental test verification has studied by Xiang and Nishitani(2015). Application of DVA to suppress unstable vibration and noise caused friction studied by Rusli *et al.* (2015). Farshidianfar and Soheili (2013) used Artificial Bee Colony (ABC) optimization in designing a TMD for tall buildings with soil structure interaction. Seto *et al.* (2011) developed an adjustable pendulum-like controller for reducing the

*Corresponding author, Professor
E-mail: mulyadibur@ft.unand.ac.id
[a]Ph.D.
E-mail: lovelyson@ft.unand.ac.id
[b]Ph.D.
E-mail: meifal@ft.unand.ac.id
[c]Professor
E-mail: mokuma@mech.titech.ac.jp

 ISSN: 2092-7614 (Print), 2092-7622 (Online)

vibration response of a three storey building.

Many methods have been developed for designing a single-degree-of-freedom (SDOF) absorber to damp SDOF vibration. However, there are few studies for the case where both the absorber and the main system have multiple degrees of freedom. Optimization of multiple tuned mass dampers (TMD) for large-span roof structures subjected to wind loads has been studied by Zhou *et al.*(2015). Zuo and Nayfeh (2004) compared three optimization techniques using minimax, H_2, and H∞ for obtaining optimum DVA parameters in reducing the vibration response of a free-free beam system. A double dynamic vibration absorber using a combination of a TMD and a pendulum to reduce the vibration response of a two-DOF shear structure has been investigated (Son *et al.* 2016a). Son *et al.* (2016b) proposed a combination of TMD and tuned liquid column damper (TLCD) absorber for suppressing the vibration of a two DOF structure. In this research, a new type of dynamic vibration absorber using a double pendulum with spring and dashpot elements for simultaneously reducing the frequency response at the 1st and 2nd resonance peak of a Two-DOF shear structure is proposed. Differ from one pendulum DVA which can only reduce one resonance peak, two pendulums DVA can reduce two resonance peaks of the frequency response. Therefore, this technique is more effective in suppressing the response of a MDOF structure under wide excitation frequency range such as the seismic excitation.

Firstly, the nominal values of DVA parameters are calculated by the Genetic Algorithm (GA) procedure. Next, a simulation study is conducted to evaluate the absorber performance as the DVA parameters such as pendulum masses (m_{d1} and m_{d2}), length of pendulums (R_1), the position of the connecting spring and dashpot(a), spring stiffness (k_d), dashpot damping coefficient(c_d) and pendulum damping coefficients (C_{d1}, C_{d2}) were varied. Finally, an experimental study is conducted to assess the DVA performance and validate the simulation results.

2. Theoretical background

2.1 The gverning euations

The model of a two DOF shear structure with two pendulums is shown in Fig. 1. The pendulums are connected to each other by a spring and dashpot element. Four beam elements with fixed-fixed boundary conditions are used for connecting the first floor to the ground and the second floor. The m_{s1} and m_{s2} denote the mass of the 1st and 2nd floor respectively, and m_{d1} and m_{d2} are the pendulum masses. The length of each pendulum is the distance from the pendulums hinges joints to the pendulum masses are denoted by R_1 and R_2, respectively. The distance of the connecting spring and dashpot element from the pendulum's hinges joint is a.

A two DOF spring-mass vibration system as shown in Fig. 2 is used to represent a simplified model of the shear structure. The dynamic vibration absorbers consist of two pendulums connected with spring and dashpot element are located in the second mass of the main system. In the

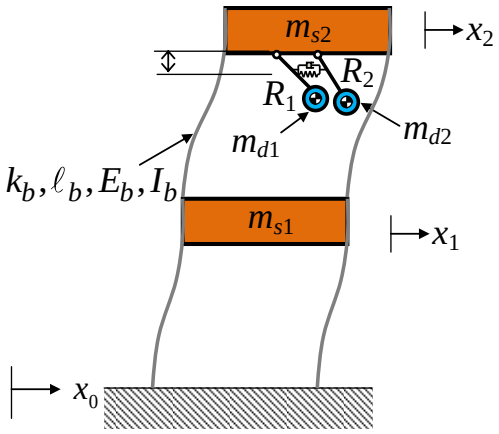

Fig. 1 Two DOF shear structure with double pendulum

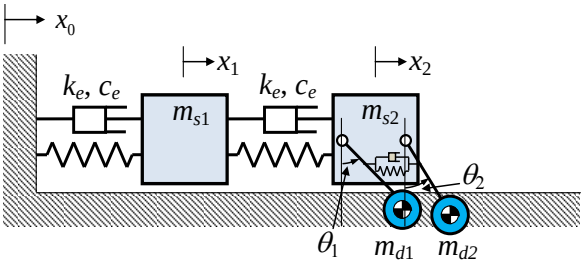

Fig. 2 Simplified model of two DOF shear structure with double pendulums

simplified model as shown in Fig. 2, the equivalent stiffness is calculated using the elastic theory of the beam elements with fixed-fixed boundary condition

$$k_e = 4 \times k_b = 4 \times \frac{12 E_b I_b}{\left(\ell_b\right)^3} \quad (1)$$

Where k_b is the stiffness of beam elements. E_b, I_b and l_b are the beam elastic modulus, moment of inertia and length, respectively. The damping coefficient c_e in Fig. 2 denotes the inherent damping of the beam elements.

The horizontal force components due to the interaction between the pendulums and the second mass ms_2 can be written as

$$F_{x1} = m_{d1}\left(R_1\ddot{\theta}_1 + \ddot{x}_2\right) - c_d a\left(\dot{\theta}_2 - \dot{\theta}_1\right) - k_d a\left(\theta_2 - \theta_1\right) \quad (2)$$

$$F_{x2} = m_{d2}\left(R_2\ddot{\theta}_2 + \ddot{x}_2\right) + c_d a\left(\dot{\theta}_2 - \dot{\theta}_1\right) + k_d a\left(\theta_2 - \theta_1\right) \quad (3)$$

where k_d and c_d are the stiffness and the damping coefficients of the spring and dashpot elements, which connect the both pendulums. When a harmonic excitation is applied at the base of the structure, the governing equation of a two DOF vibration system with two pendulums can be expressed by

$$\begin{bmatrix} m_{s1} & 0 & 0 & 0 \\ 0 & m_{s2}+m_{d1}+m_{d2} & m_{d1}R_1 & m_{d2}R_2 \\ 0 & m_{d1}R_1 & m_{d1}R_1^2 & 0 \\ 0 & m_{d2}R_2 & 0 & m_{d2}R_2^2 \end{bmatrix} \begin{Bmatrix} \ddot{x}_1 \\ \ddot{x}_2 \\ \ddot{\theta}_1 \\ \ddot{\theta}_2 \end{Bmatrix} + \begin{bmatrix} 2c_e & -c_e & 0 & 0 \\ -c_e & c_e & 0 & 0 \\ 0 & 0 & c_d a^2 + C_{d1} & -c_d a^2 \\ 0 & 0 & -c_d a^2 & c_d a^2 + C_{d2} \end{bmatrix} \begin{Bmatrix} \dot{x}_1 \\ \dot{x}_2 \\ \dot{\theta}_1 \\ \dot{\theta}_2 \end{Bmatrix} \quad (4)$$

$$+\begin{bmatrix} 2k_e & -k_e & 0 & 0 \\ -k_e & k_e & 0 & 0 \\ 0 & 0 & m_{d1}gR_1 + k_d a^2 & -k_d a^2 \\ 0 & 0 & -k_d a^2 & m_{d2}gR_2 + k_d a^2 \end{bmatrix} \begin{Bmatrix} x_1 \\ x_2 \\ \theta_1 \\ \theta_2 \end{Bmatrix} = \begin{Bmatrix} k_e \\ 0 \\ 0 \\ 0 \end{Bmatrix} X_0 \sin \omega t$$

or

$$[\mathbf{M}]\{\ddot{\mathbf{x}}\} + [\mathbf{C}]\{\dot{\mathbf{x}}\} + [\mathbf{K}]\{\mathbf{x}\} = \{\mathbf{f}\} \tag{5}$$

The damping components at each pendulum hinge joint are denoted by C_{d1} and C_{d2}. The governing equation in (5) can be written in the modal coordinate as follows

$$[\mathbf{m_r}]\{\ddot{\mathbf{q}}\} + [\mathbf{c_r}]\{\dot{\mathbf{q}}\} + [\mathbf{k_r}]\{\mathbf{q}\} = \{\mathbf{p}\}\ ,\ \{\mathbf{q}\} = [\mathbf{\Phi}]^{-1}\{\mathbf{x}\} \text{ and } \{\mathbf{p}\} = [\mathbf{\Phi}]\{\mathbf{f}\}$$

or

$$m_r \ddot{q}_r + c_r \dot{q}_r + k_r q_r = p_r \ ,\ r = 1, 2, \cdots, N \tag{6}$$

where $\mathbf{\Phi}$, $\mathbf{m_r}$, $\mathbf{c_r}$ and $\mathbf{k_r}$ are the eigenvector, modal mass, modal damping and modal stiffness of the system, respectively. The frequency response function (FRF) is calculated as a ratio between the response signal and the excitation signal as given by

$$\alpha_{jk}(\omega) = \sum_{r=1}^{N} \frac{(\Phi_{jr})(\Phi_{kr})}{(k_r - \omega^2 m_r) + i(\omega c_r)} \tag{7}$$

2.2 Genetic algorithm

A genetic algorithm(GA) is a stochastic global search technique (Haupt 2004) based on the evolution theorem. This optimization technique can be used in a wide range of problems even when the function cannot be optimized analytically.

In GA optimization an objective function is selected. In this case, the objective function is formed from the frequency response function of the system as given in Eq. (7). The main step in the GA optimization process is the evaluation of the objective function. The evaluation is performed to each chromosome in the population. The population is modified using the GA operators of selection, crossover and mutation to obtain the fittest chromosome according to specified criteria (Son *et al*. 2016a).

3. Numerical study

The nominal values of the simulation parameters are listed in Table 1. The nominal parameters of the pendulum such as R_1, R_2, a, c_d, C_{d1} and C_{d2} are calculated based on the GA optimization procedure. In the optimization process, the connecting spring stiffness k_d and the pendulum mass m_d are not optimized but selected manually. The optimum parameters of DVA are calculated by GA as follows:

$$\text{Minimize}: \ G(R_1, R_2, a, c_d, C_{d1}, C_{d2})$$

$$\text{Subject to}: \ 0.05 \le R_1 \le 0.2\,, \quad 0.05 \le R_2 \le 0.2\,,$$

$$0.04 \le a \le 0.01$$

$$0 \le c_d \le 0.001\,, \quad 0 \le C_{d1} \le 0.001\,, \quad 0 \le C_{d2} \le 0.001$$

Table 1 Nominal parameters in simulation

No	Parameters	Value
1	Mass of the 1st floor (M_{s1})	3.035 kg
2	Mass of the 2nd floor (M_{s2})	3.010 kg
3	Structural stiffness (k_e)	1.64×10^3 N/m
4	Pendulum masses (m_{d1} and m_{d2})	0.2 kg
5	Stiffness (k_d)	300 N/m
6	Damping coefficient (c_d)	1×10^{-3} Ns/m
7	Length of the 1st pendulum (R_1)	0.053 m
8	Length of the 2nd pendulum (R_2)	0.058 m
9	Position of the spring/dashpot (a)	0.035 m
10	Pendulum damping (C_{d1} and C_{d2})	1×10^{-3} Nms

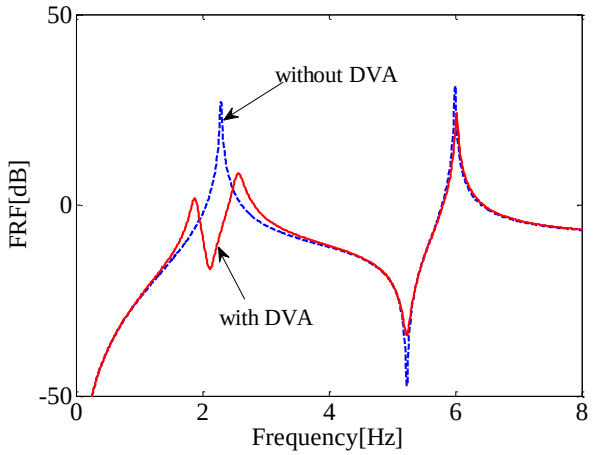

Fig. 3 Result of point FRF at the second floor

$$k_d = 300 \ \text{ and } \ m_d = 0.2$$

Since there are two natural frequencies of the structure, two functions f_1 and f_2 corresponding to the cost function calculated in the regions closest to the 1st and the 2nd natural frequency are combined into a single objective function G (Son *et al.* 2016a)

$$G = \alpha f_1 + (1-\alpha) f_2\,; \qquad \alpha \in [0\ 1] \tag{18}$$

For the parametric study, the FRF is calculated based on the ratio between vibration response and the excitation signal in modal coordinates as given in Eq. (7). In the FRF calculation, modal damping of the structure for the first and second mode are selected to be 0.005 and 0.001, respectively. The nominal values of structure and DVA parameters as depicted in Table 1 are used in the simulation. The DVA parameters in Table 1 are calculated using Genetic Algorithm (GA) procedure.

The structural response with and without DVA is depicted in Fig. 3. As shown in Fig. 3, double peaks occurred near the first natural frequency of the structure with DVA. The magnitudes of these peaks are lower than without DVA ones. In the region located near the second natural frequency of the structure, attenuation of the FRF peak in the model with DVA can be clearly observed. This is possibly caused by an additional damping factor from the pendulums' hinge joints.

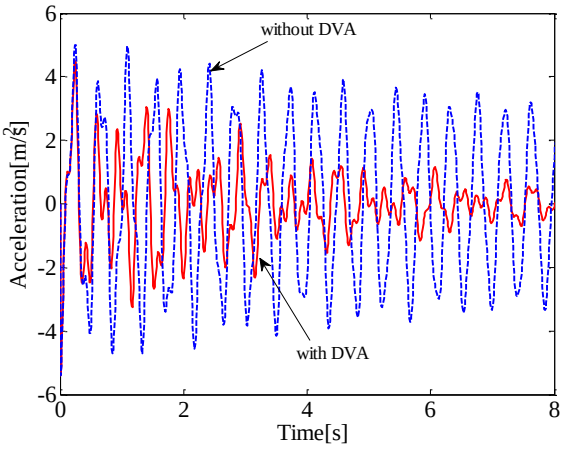

Fig. 4 Free vibration response from the simulation

The free vibration response is calculated to investigate the performance of the absorber in reducing the acceleration response of the structure due to the initial displacement applied to the floor mass. Fig. 4 shows the structure response at the second floor for two cases; without DVA and using DVA. The initial displacement of the first and the second floor are selected to be 0.01 and 0.02 m, respectively. To obtain comparable results to experimental data, the damping coefficients of the structure and the pendulums' hinge joints are selected to be c_e=0.5 Ns/m and C_{d1}=C_{d2}=5×10^{-4} Nsm, respectively. It can be observed from Fig.4 that the amplitude of the acceleration response of the structure with DVA decreases faster than without DVA one.

The parametric study is conducted to investigate the effect of variations in the parameters on DVA performance. The evaluation is performed on the absorber parameters such as the damper masses (m_{d1}, m_{d2}), the first damper mass position (R_1), connecting spring and dashpot position(a), connecting spring stiffness(k_d), connecting dashpot damping coefficient (c_d) and the pendulum's hinge joints damping coefficient (C_{d1}, C_{d2}).

3.1 The pendulum mass variation (m_{d1}, m_{d2})

The simulation is performed by making the first and the second damper mass are equal (m_{d1} = m_{d2} = m_d). The damper masses vary from 0.1 to 2 times of the nominal value as depicted in Table 1. Fig. 5 shows the effect of damper mass variation on the FRF of the system. As shown in Fig. 5, the increasing of the damper mass significantly affects the frequency response of the system. At the first natural frequency region (2.2 Hz), the FRF curve changes drastically responding to the variations of the damper mass. Meanwhile, in the region closest to the second natural frequency (6 Hz), small difference in the FRF peaks is detected when the damper mass is varied from 0.1 to 2 times the nominal value.

3.2 The pendulum length (R_1)

Fig. 6 shows the effect of the first pendulum length (R_1) to the FRF of the system. In this simulation, the pendulum length is varied from 1 to 1.8 times of its nominal value. As

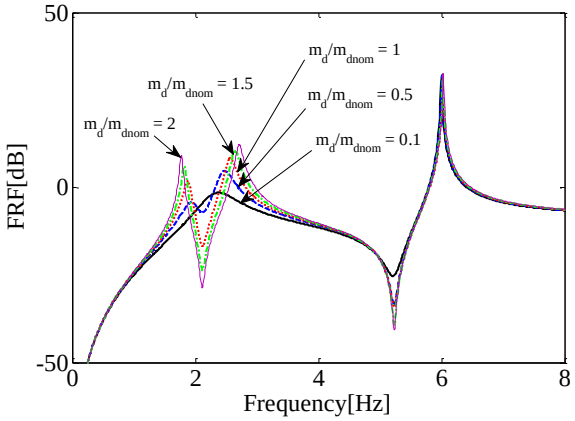

Fig. 5 Variation of FRF vs damper mass weight

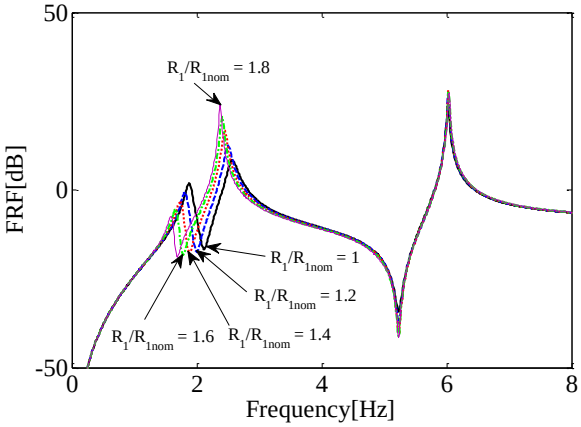

Fig. 6 Variation of FRF vs R_1

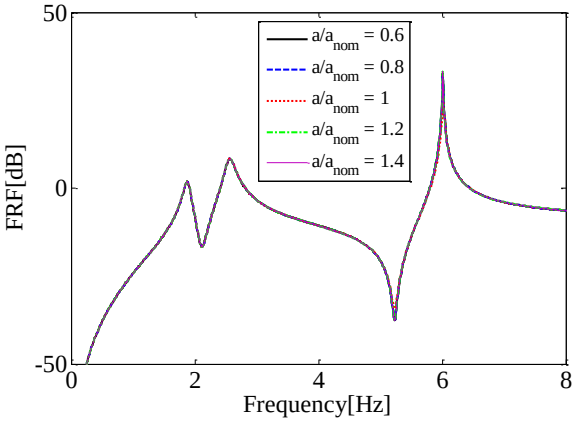

Fig. 7 Variation of FRF vs a

can be shown in Fig. 6, variations of R_1 significantly change the FRF peak position near to the first natural frequency of the system. However, the FRF peaks of the second natural frequency are not much affected by the pendulum length as shown in Fig. 6.

3.3 The connecting spring and dashpot position(a)

The connecting spring and dashpot position (a) is measured from the pendulum's hinge joint as shown in Fig. 1. To investigate the effect of connecting spring and dashpot

position, the simulation of FRF using several spring and dashpot positions is conducted. The variation range of a is $0.6\ a_{nom} \leq a \leq 1.4\ a_{nom}$ where a_{nom} is the nominal value of a as shown in Table 1. Fig. 7 shows that FRF of the system near the first natural frequency (2.2 Hz) is not much affected by variation of the spring and dashpot position. However, some changes in magnitude in the FRF peak near to the second natural frequency (6 Hz) are observed when the spring and dashpot position is varied from 0.6 to 1.4 times of its nominal value.

3.4 The connecting spring stiffness (k_d)

The connecting spring stiffness then is varied according to $0.5\ k_{dnom} \leq k_d \leq 8\ k_{dnom}$ as depicted in Fig. 8. As shown in Fig. 8, the FRF curves change very little when the spring stiffness is varied from 0.5 to 8 times of its nominal value. Furthermore, in the region closest to the second natural frequency (6 Hz), only slight changes in FRF level are detected for different values of k_d.

3.5 The connecting dashpot damping coefficient (c_d)

Fig. 9 shows variations in the FRF of the system versus the damping coefficient c_d. In the simulation, the damping coefficient is varied within the range of $c_{dnom} \leq c_d \leq 16 c_{dnom}$. The FRF curve is almost equal when the damping coefficient is increased up to 16 times of its nominal value. These results indicate that the damping coefficient c_d has no significant role in pendulum type of DVA design.

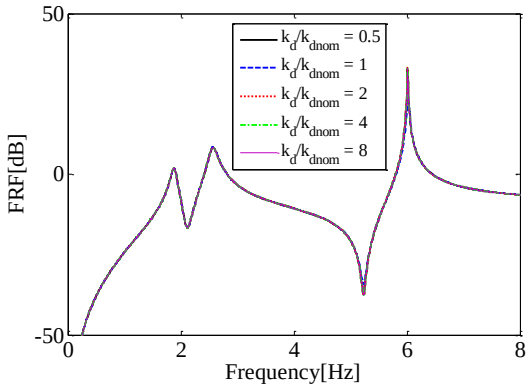

Fig. 8 Variation of FRF vs k_d

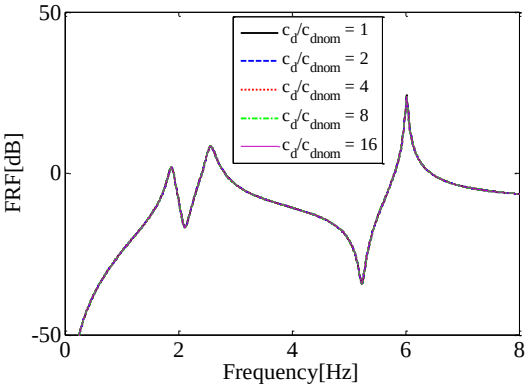

Fig. 9 Variation of FRF vs c_d

3.6 The Pendulum damping coefficient (C_{d1},C_{d2})

Moreover, to investigate the effect of pendulum's hinge joints damping coefficient, the values of C_{d1} and C_{d2} then are varied. The left and the right pendulum damping coefficient are assumed to be same ($C_{d1}=C_{d2}=C_d$). Fig. 10 shows the relation between the system FRF and the damping coefficient of the pendulum's hinge joints. It is shown that the pendulum's hinge joint damping coefficients have a significant role in reducing the FRF peaks and become an important factor in pendulum type DVA design. The increasing of the pendulums' damping coefficient reduces the magnitude of the FRF peak near the resonance frequency (2.2 Hz and 6 Hz).

3.7 Time domain analysis under seismic excitation

The attenuation of the acceleration response due to the addition of the pendulum damping coefficient is not investigated only when the structure is excited by a harmonic excitation, but also observed in the time domain. Fig. 11 shows the acceleration response of the structure under a seismic excitation that matching of the El-Centro earthquake at the base of the structure. It can be observed that increasing the pendulum damping coefficient causes the reduction in the acceleration response of the structure.

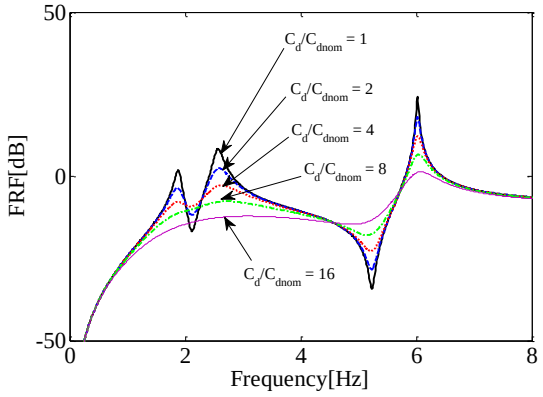

Fig. 10 Variation of FRF vs C_d

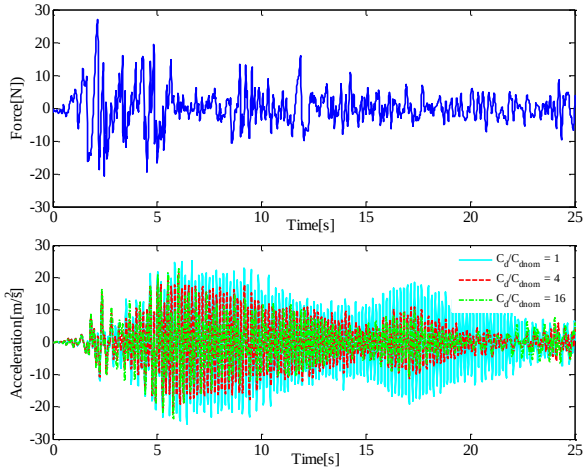

Fig. 11 Acceleration response under El-Centro earthquake excitation

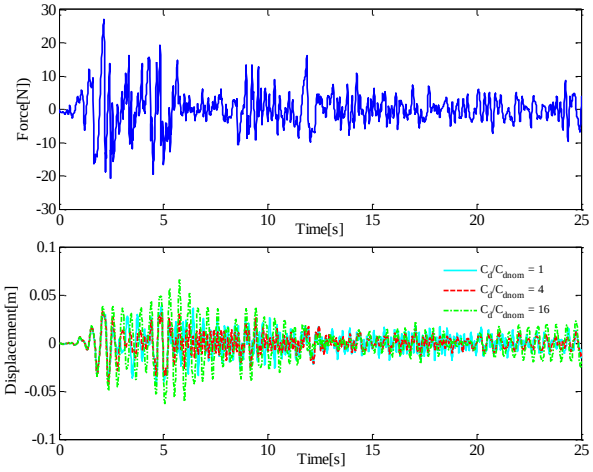

Fig. 12 Displacement response under El-Centro earthquake excitation

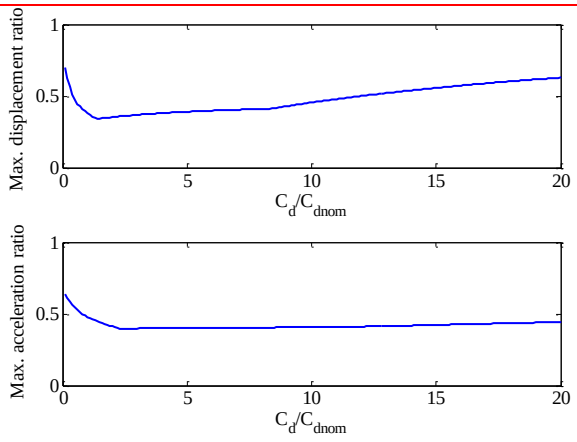

Fig. 13 Maximum displacement and acceleration ratio vs C_d

The displacement response at the second floor calculated by numerical simulation using different values of the pendulum damping coefficient is depicted in Fig. 12. It is shown that the displacement response decreases when the damping coefficient increases four times of its nominal values. However, when the damping coefficient is 16 times of its nominal value, the displacement response increases more than that original one. This result indicates that the application of large damping coefficient is not an effective way for reducing the displacement response of the structure.

The relation between the maximum displacement ratio and the maximum acceleration ratio to the pendulum damping coefficient is depicted in Fig. 13. The displacement and acceleration ratio are the ratio between the maximum structure response with and without the absorber. The optimum condition for the pendulum damping coefficient is located near to C_d=2C_{dnom}.

4. Experimental study

The experimental model of DVA consists of two rigid beams as the pendulum bars that have a guide hole which is used to change the position of the pendulum mass and a

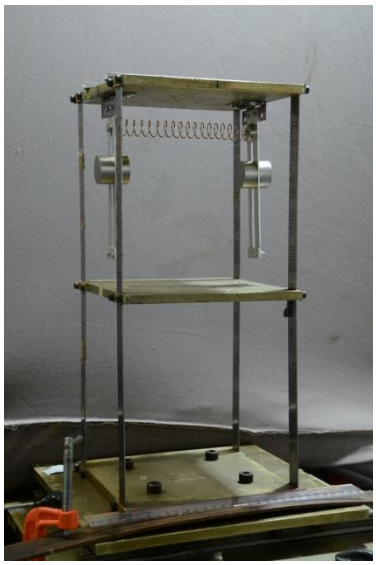

Fig. 14 Experimental model

connecting spring as shown in Fig. 14. The length of the guide hole is 0.2 m. Theoretically, the pendulum length and the spring position can be adjusted from 0 to 0.2 m. However, because of some technical limitations regarding to the dimension of the pendulum mass and connecting spring, the minimum position of the connecting spring and the pendulum length are 0.015 m and 0.03 m, respectively.

The damping coefficient of the pendulums and the connecting dashpot are not adjusted during the experimental study. The weight of the pendulum mass is 0.2 kg, which is the same as the nominal pendulum mass as shown in Table 1. The pendulum length and the spring position are adjusted around the nominal position as depicted in Table 1.

The experimental study is conducted using the National Instrument data acquisition system. The acceleration data are measured using an ICP piezoelectric accelerometer. For the frequency response function (FRF) measurement, the impact excitation is applied using an Impact hammer. Point FRF measurement is used to validate the simulation data. In this case, the accelerometer position and the excitation point of the impact hammer is located on the second floor of the structure.

Fig. 15 shows the experimental result of FRF without the DVA. It can be observed that the level of experiment resonance peaks at 2 Hz and 6 Hz are lower than those obtained in simulations as shown in Fig. 3. This possibly due to the fact that the minimum frequency line used for FRF calculation in the experiment was limited to 0.25 Hz. Therefore, the peak resonances are lower than those obtained in the simulation.

Fig. 16 shows some point FRFs measured at the second floor of the structure with DVA. These FRFs are obtained using different pendulum lengths (R_1 and R_2). It can be seen that the experimental results are matched with those obtained by the simulations. Because the pendulum damping effects are negligible and kept constant during the experiment, there is no significant change in the resonance peak in the second natural frequency.

Furthermore, Fig. 16 shows that double peaks occur

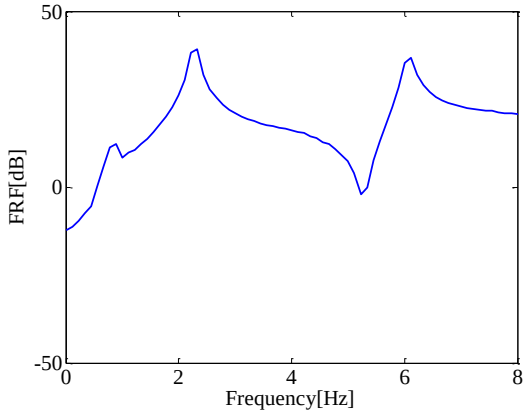

Fig. 15 FRF structure without DVA at the second floor

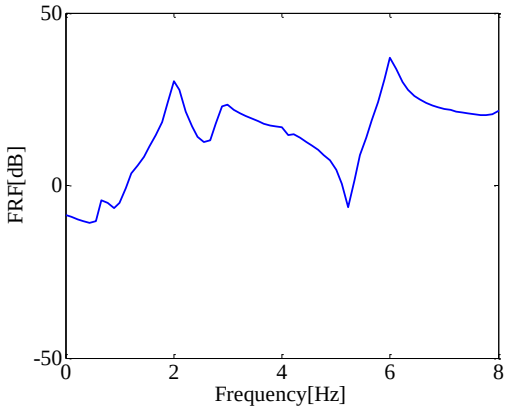

(a) R_1=R_2=6 cm

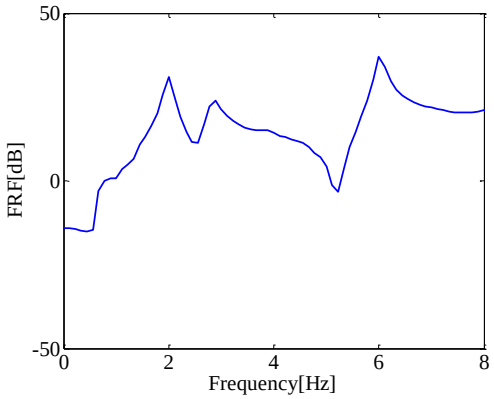

(b) R_1=R_2=6.5 cm

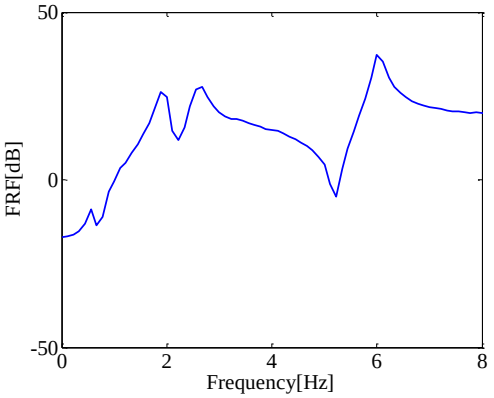

(c) R_1=R_2=8 cm

Fig. 16 Experimental results of point FRF at the second floor

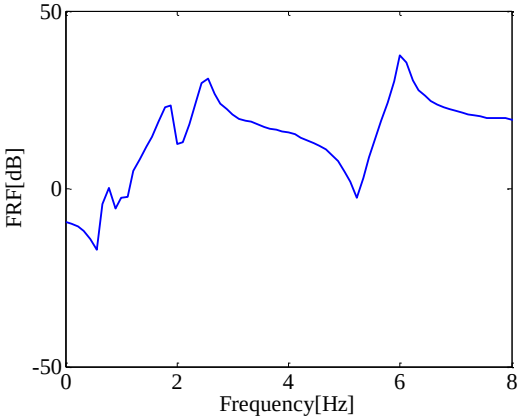

(d) R_1=R_2=10 cm

Fig. 16 Continued

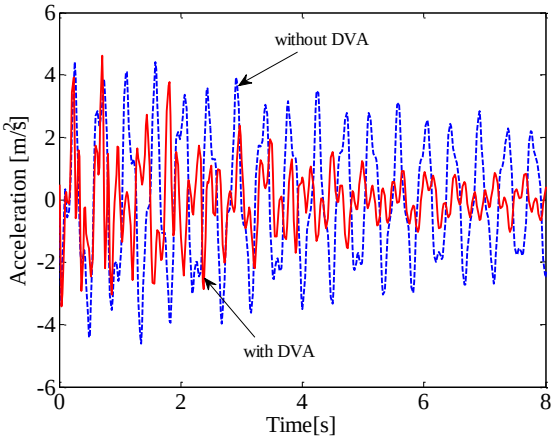

Fig. 17 Free vibration response from the experiment

near to the first natural frequency of the structure. These two peaks level change with the length of the pendulums and have the same level when the both pendulums lengths are 8 cm. These results are slightly different from the nominal pendulum length used in the simulation. The difference may be caused by the addition of mass from the pendulum bars in the experiment which is not considered in the numerical simulation.

Moreover, a comparison of free vibration responses of the structure at the second floor between without DVA and with DVA is shown in Fig. 17. The initial displacements of the first and the second floor in the experimental study is selected to be the same as those used in the simulation. The pendulums are both 8 cm lengths. The experimental result agrees very well with the numerical simulation result as shown in Fig. 4.

5. Conclusions

This study investigates the properties of a new type of dynamic vibration absorber using a double pendulum connected with spring and dashpot element to reduce the vibration response of a two DOF vibration system. A mathematical model of the structure with the dynamic

absorber is derived and a parametric study is performed to evaluate the effect of the DVA parameters to its performance. It is found that the pendulum length (R_1, R_2), mass (m_d) and the pendulum damping coefficient (C_{d1}, C_{d2}) significantly affects the DVA performance, but the connecting spring stiffness (k_d), the damping coefficient of the dashpot (c_d), and the spring position (a) give no influence to reduce the vibration response. The experimental study assesses the DVA performance. The experimental study assessed the DVA performance. The experimental results agree very well with the results of those obtained in the simulations indicating the validity of the simulation and the GA optimization solutions obtained.

Acknowledgments

The authors gratefully acknowledge the financial support by Hibah Klaster Riset Guru Besar from Andalas University with contract number 104/UN.16/HKRGB/LPPM/2016.

References

Bayramoglu, G., Ozgen, A. and Altinok, E.(2014), "Seismic performance evaluation and retrofitting with viscous fluid dampers of an existing bridge in Istanbul", *Struct. Eng. Mech*, **49**(4), 463-477.

Farshidianfar, A. and Soheili, S. (2013), "ABC optimization of TMD parameters for tall buildings with soil structure interaction", *Inter. Multi. Mech*., **6**(4), 339-356.

Fosdick, R. and Ketema, Y. (1998), "A thermoviscoelastic dynamic vibration absorber", *J. Appl. Mech*., **65**(1), 17-24.

Gong, X., Peng, C., Xuan, S., Xu, Y. and Xu, Z. (2012), "A pendulum-like tuned vibration absorber and its application to a multi-mode system", *J. Mech. Sci. Tech.*, **26**(11), 3411-3422.

Haupt, R.L. and Haupt, S.E. (2004), *Practical Genetic Algorithm*, John Willey & Sons, USA.

Mizuno, T. and Araki, K. (1993), "Control system of a dynamic vibration absorber with an electromagnetic servomechanism", *J. Mech. Syst. Sig. Proc.*, **7**(4), 293-306.

Ni, P. (2014), "Seismic assessment and retrofitting of existing structure based on nonlinear static analysis", *Struct. Eng. Mech.*, **49**(5), 631-644.

Rusli, M., Bur. M. and Son, L. (2015), "Dynamic vibration absorber for squeal noise suppression in simple model structures", *Int. J. Struct. Stab. Dyn.*, **15**(5), 1450078.

Salazar, A.R., Beltran, F.V., Escobedo, D.D., Mora, E.B. and Barraza, A.L. (2016), "Combination rules and critical seismic response of steel buildings modeled as complex MDOF systems", *Earthq. Struct.*, **10**(1), 211-238.

Seto, K., Iwasaki, Y., Shimoda, I., Oda, S. and Watanabe, T. (2011), "Vibrataion control for house structures beyond 3 story using pendulum-type controller underground excitation like traffic vibrations or earthquakes", *J. Syst. Des. Dyn.*, **5**(5), 653-664.

Shariatmadar, H. and Razavi, H.M. (2014), "Seismic control response of structures using an ATMD with fuzzy logic controller and PSO method", *Struct. Eng. Mech.*, **51**(4), 547-564.

Son, L., Bur, M. and Rusli, M.(2016b), "Response reduction of Two DOF shear structure using TMD and TLCD by considering absorber space limit and fluid motion", *Appl. Mech. Mat*., **836**, 251-256.

Son, L., Bur, M., Rusli, M. and Adriyan, A. (2016), "Design of double dynamic vibration absorbers for reduction of two DOF vibration system", *Struct. Eng. Mech.*, **57**(1), 161-178.

Wang, L., Liang, S., Song, J. and Wang, S. (2015), "Analysis of vortex induced vibration frequency of super tall building based on wind tunnel tests of MDOF aero-elastic model", *Wind Struct.*, **21**(5), 523-536.

Xiang, P. and Nishitani, A. (2015), "Optimum design and application of non-traditional tuned mass damper toward seismic response control with experimental test verification", *Earthq. Eng. Struct. D.*, **44**(13), 2199-2220.

Yamada, K. (2015), "Enhancing efficiency of piezoelectric element attached to beam using extended spacers", *J. Sound Vib.*, **341**(1), 31-52.

Zhang, C., Zhou, Y., Weng, D.G., Lu, D.H. and Wu, C.X. (2015), "A methodology for design of metallic dampers in retrofit of earthquake-damaged frame", *Struct. Eng. Mech.*, **56**(4), 569-588.

Zhou, X., Lin, Y. and Gu, M. (2015), "Optimization of multiple tuned mass dampers for large-span roof structures subjected to wind loads", *Wind Struct.*, **20**(3), 363-388.

CC